A Novel Approach for Image Fusion through Hybrid Transforms Technique

Dr. Jyoti S. Kulkarni , Assistant Professor, Pimpri Chinchwad College of Engineering, Pune, India

jyoti.kulkarni@pccoepune.org

Abstract **The sensors available nowadays are not generating images of all objects in a scene with the same clarity at various distances. The progress in sensor technology improved the quality of images over recent years. However, the target data generated by a single image is limited. For merging information from multiple inputs, image fusion is used. The basis of fusion is on the image acquisition as well as on the level of processing and under this many image fusion techniques are available. The fusion methods are divided into two domains i.e. spatial and frequency domains. The fusion in spatial domain images uses inputs directly to work on pixels, while the transition refers to frequency domain image fusion on input images before fusion. The limitation of spatial domain image fusion is spectral degradation. To overcome this limitation, the fusion of transform domain images is preferred. The results generated by transform methods are superior to spatial domain methods. But by the analysis of the transform domain, there is a scope to improve the results or to find the optimized results. By combining the spatial domain and transform domain technique, the hybrid transform technique is proposed where HSV transform from the spatial domain, and any of the transform methods are combined. The result obtained by the proposed technique is compared with existing transform methods and observed that the results are improved. The performance parameters are used to find degradation in the image tested on four types of input sets by the three different modes.**

Keywords — HSV, HDWT, HDCT, HKT, HDST, HWT .

I. INTRODUCTION

Image fusion is accomplished in four different stages. These levels are the level of the signal, pixel level, level of feature, and level of decision-making. At the signal level, signals from different sensors are combined to create a new signal. Pixel level image fusion works for the pixel value to boost the efficiency of the fused data. Feature level uses the salient features of the image like size, shape, edge, pixel intensity, and texture before fusion. At the decision level, a necessary judgment on integrating the information is taken before the fusion [9, 10]. The fusion methods are split into spatial domains and frequency domains. The fusion of spatial domain images uses inputs directly to work on pixels, while the transition refers to frequency domain image fusion on input images before fusion. Depending on the availability of reference images, the performance parameters are divided into two categories: reference parameters and no reference parameters. The root means squared error (RMSE), peak signal to noise ratio (PSNR), mutual information (MI), and structural similarity index metrics are available as the reference parameters whereas mean, entropy, standard deviation, spatial frequency (SF), average gradient (AG), and fusion mutual information are used as the no reference parameters.

Image fusion is done at three different levels. These levels are pixel level, feature level, and decision-making level. Pixel level fusion works on pixel values. Feature level image fusion uses the features like size, shape, edge, pixel intensity, and texture before fusion. At the decision level, a suitable decision about integrating the information is taken prior to the fusion. The image fusion methods are distributed into the spatial domain and frequency domain. The spatial domain image fusion directly operates on pixels whereas frequency domain image fusion transforms the input images before image fusion. The spatial domain image fusion methods include an averaging method, Principal Component Analysis (PCA), Intensity Hue Saturation (IHS) transform, High Pass Filtering, and Brovey Transform.

In the averaging image fusion method, an average of the corresponding pixels in every input image is used in the resultant image. This is a very basic and simple image fusion technique. Similar to this technique, the maximum pixel value technique, minimum pixel value technique, and max-min technique are available which use maximum, minimum, and average of the higher and lower value respectively of the corresponding pixels of input image [4]. The PCA is the transformation of intercorrelated multispectral bands into mutually independent elements.

This is accomplished by finding the principal components of the multispectral image. As the first component contains the most information, this component is replaced by a panchromatic image. The fused image is formed after taking the inverse transform of the resultant image [10].

IHS transform uses IHS color space. Similar to the PCA method, the multispectral image is converted from RGB to IHS. This gives three bands; Intensity, Hue, and Saturation. The intensity band is replaced by a panchromatic image. Now three bands are available i.e. modified intensity, hue, and saturation. Now inverse IHS transform is applied to this image gives the fused image of multispectral RGB bands [10]. High pass filtering image fusion consists of the addition of spatial details from a high and low-resolution image. Low-resolution image already consists of spatial information whereas high-frequency spatial data is obtained by filtering the multispectral image through a simple local pixel averaging method. The Brovey transform-based image fusion is a ratio method where the data values of each band of image 1 are divided by the sum of the data set of image 1 and then multiplied by the image 2 data set [10]. The limitation of each spatial domain image fusion method is spectral degradation. To overcome this limitation, transform domain image fusion is preferred. The transform domain image fusion method uses different transforms such as discrete cosine transform (DCT) [5, 8, 13, and 20], discrete sine transform (DST) [16], discrete wavelet transform (DWT) [3, 22, 31, and 36], Walsh transforms (WT) [14, 57], and Kekre transforms (KT) [4].

II. LITERATURE SURVEY

Dammavalam *et al.* [11] proposed fuzzy logic-based pixel-level image fusion. Fuzzification, membership modification and defuzzification are three steps involved in fuzzy image processing. In fuzzification, the images are encoded and in defuzzification, the output image is decoded. The appropriate membership function and modification is used to fuse the images appropriately. This technique can be further extended using neuro-fuzzy logic. Aithal *et al.* [12] analyzed multiresolution image fusion, the smoothing filter-based intensity modulation. This is represented by a digital number that is dependent on irradiance and the ground surface spectral reflectance. This is designed for urban extension analysis. He *et al.* [18] explained the multifocus image fusion by training the cascade forest model. The results are predicted from this model. The selection of the final decision map is done by the guided filter.

Zhao *et al.* [22] suggested a hybrid principal component analysis approach to image fusion of terahertz and visible images. Two-step image fusion is performed in the proposed method. Initially, PCA based image fusion is performed on input images by finding the principal component transformation matrix of the visible image. In the second step, the visible image is transformed into IHS space. The fused PCA and I channel are fused to get a new luminance component. The inverse of this component with the H and S channel gives the final fused image. For multispectral and hyperspectral data fusion, a coupled nonnegative matrix factorization unmixing was suggested by Yokoya *et al.* [23]. Applying NMF unmixing on input images produces high spatial resolution abundance and hyperspectral endmember matrices. These two matrices give fused data. Zhaoyang *et al.* [27] suggested robust image fusion approach for image misregistration. The multimodal logistic regression classifier and random walker optimization are two main parts of the proposed method. The classifier is used for feature extraction and parameter analysis whereas random walker optimization is used for segmentation. This method gives less computational efficiency.

Benjamin *et al.* [30] introduce a new form of fusion by combining optical and digital techniques. The optical technique works in the specified depth of field to acquire the high-resolution focused image. The digital technique fuses the images by using the principal component analysis method. This method can be extended by using segmentation before the PCA method. Farid *et al.* [31] proposed a content-adaptive blurring algorithm for the merging of multifocus inputs. This process is split into three parts. Initially, the focused region is detected by the proposed algorithm. The graph cut and morphological operations are used for segmentation. Finally, pixel-based fusion is done.

Amolins *et al.* [1] described the wavelet-based image fusion method. Here, wavelet transformation is applied on panchromatic (PAN) high-resolution images and multispectral (MS) low-resolution images. Detailed MS image information is replaced by detailed PAN image information. Inverse transformation of wavelets is done to MS input to obtain the high-resolution multispectral image. The additive wavelet fusion scheme is also explained here. This is the combination of the IHS transform and wavelet fusion method. The spatial and spectral performance is given by the IHS transform and wavelet fusion method respectively. Jinju *et al.* [6] also proposed spatial frequency DWT-based multiresolution image fusion. DWT is applied to input images to get detailed and approximation coefficients. The approximation coefficient of the panchromatic image is substituted by approximation coefficients of multispectral coefficients. The spatial frequency of detailed coefficients of both the images is calculated. The fused detailed coefficient is calculated. The inverse DWT on

approximation and detailed coefficients give the fused image.

Bhatnagar *et al.* [2] presented a novel method in the domain of the wavelet packet. This is by using directive contrast and median parameters. Input data are subdivided into coefficients of high and low-frequency. The directive contrast of horizontal, vertical, diagonal components of the high-frequency band and a low-frequency median approximate component forms the resultant image. Applying inverse discrete wavelet packet transform on a resultant image produces the fused image. Naidu [20] has explained six types of DCT based algorithms for image fusion. These are selecting coefficients by DCT averaging, DCT maximum, lowest magnitude DCT, largest contrast measure DCT, and DC coefficients. These algorithms are used in real-time applications.

Lewis *et al.* [7] proposed complex wavelet transform for region-based data merging. On the inputs, the dual-tree complex wavelet transform is applied which gives the wavelet factors. By using the rule of maximum selection, the wavelet factors are chosen for fusion. This method includes the ability to work differently on the properties such as size, average activity, and the relative position of other regions. Phamila *et al.* [8] proposed a multi-focus type for visual sensor networks using DCT. In the discrete cosine transform domain, alternating current coefficients are determined. The higher value coefficient is selected for image fusion. This method does not use complex floating-point operations and hence more energy efficient. Similarly, the images from multi exposed image sensors are fused by DCT based HDR exposure fusion. In this, the quantization process is used in JPEG encoding to measure the image superiority and preserve the naturalness. This is suitable for object identification with fast computation time and less memory requirements. [13].

Shangzheng *et al.* [15] proposed a new method using polyharmonic local sine transformation. The input image is divided into the polyharmonic and residual components. A polyharmonic component represents the base whereas the residual component represents the texture information of the input. The weighted averaging is used to merge these components. Another way to use sine transform is given by Naidu *et al.* [16]. The RGB image is converted to IHS and then fusion is done at intensity level. By using multiresolution sine wave transform for image fusion, there is no information loss. The results generated are similar to the results by discrete wavelet transform. Xia *et al.* [17] proposed a pulse coupled neural network-based multimodal image fusion technique for medical data. The non-subsampled shearlet transform is applied to the input images. This will decompose the image into coefficients of high frequency and low-frequency. The pulse-coupled

neural network is used to combine the high-frequency coefficients. The convolutional sparse representation is used to fuse the low-frequency coefficients. This is useful in multifocus and infrared-visible image fusion.

The hybrid method is suggested by Agrawal *et al.* [19]. This is the combination of wavelet and curvelet transforms. Initially, curvelet features are obtained by using ridgelet transform. The final fusion is done at the wavelet transform level. The curvelet transforms is superior in curved details to the wavelet transform. The fused image obtained using hybrid transform is better than individual transforms. Paul *et al.* [21] proposed image fusion in the gradient domain for multiexposure and multi-focus images. This method works separately on the luminance and chrominance part of the input images. The luminance part is obtained by using Haar wavelet decomposition of input luminance parts whereas the chrominance part is obtained by weighted sum on input chrominance parts.

Syed *et al.* [24] proposed a hybrid image fusion method. This works on the principle of component substitution and additive wavelet. This method preserves the radiometric and geometric information in images. Lohit *et al.* [25] proposed a trained convolutional neural network with an unrolled projected gradient descent method for multispectral image fusion. This is designed to solve the problem of fusing low-resolution and high-resolution images. The solution for this problem is also given by Shen *et al.* [26]. They have proposed a double optimization net with the decomposition of the matrix. Initially, the problem is transformed into a spectral and spatial optimization problem. These problems are solved simultaneously through the linear equation. Xie *et al.* [28] also proposed the merging of hyperspectral and multispectral inputs using a convolutional neural network. This method uses all parameters in deep learning for training the data set. Fang *et al.* [29] proposed multi-task optimization in the image fusion method. This method is designed by considering the human visual characteristics. The features are selected by using a nonlinear convolutional neural network and then multitask loss function is designed for a semi-supervised learning network for image fusion. This can be extended for self-learning image fusion also.

III. IMAGE FUSION USING HYBRID TRANSFORMS

By combining the spatial domain and transform domain technique, the hybrid transform technique is proposed. In the proposed technique, the HSV transform from spatial domain and any of transform among the DCT, DST, DWT, WT, and KT from transform domain is combined. The resultant techniques are hybrid DCT (HDCT), hybrid DST (HDST), hybrid DWT (HDWT), hybrid WT (HWT), and hybrid KT (HKT). The result obtained by the proposed technique is compared with existing transform methods

and observed that the results are improved. The block schematic of the transform-based pixel-level image fusion process is represented in Fig. 1 and Fig. 2. The input images can be either color or grayscale. To perform image fusion effectively, two different algorithms are used for color and grayscale images. Fig. 1 is the multisensor color image fusion process while Fig. 2 is the image fusion process for other types of images. In multisensor RGB image fusion, RGB colormap is converted into HSV colormap. Fig. 1 represents the block schematic for image fusion using a transform technique for multisensor RGB input images. The input multisensor RGB images are converted to HSV where the separate H, S, V bands are available. A 2D transform is applied to each band and the average gradient of each band is calculated. By applying the maximum fusion rule on each band, the band with a higher average gradient is selected. And then applying inverse transform on each selected band, H, S, V bands of the fused image are available. Converting HSV to RGB, a fused image is available. Fig. 2 represents the image fusion using a transform technique for multi-focus RGB or grayscale input images. If it is an RGB image then 2D transform is applied on each band else 2D transform is applied on the grayscale image. Then by applying the maximum fusion rule, the pixel of a higher pixel value is selected.   Then applying the inverse transform, the resultant image is obtained.
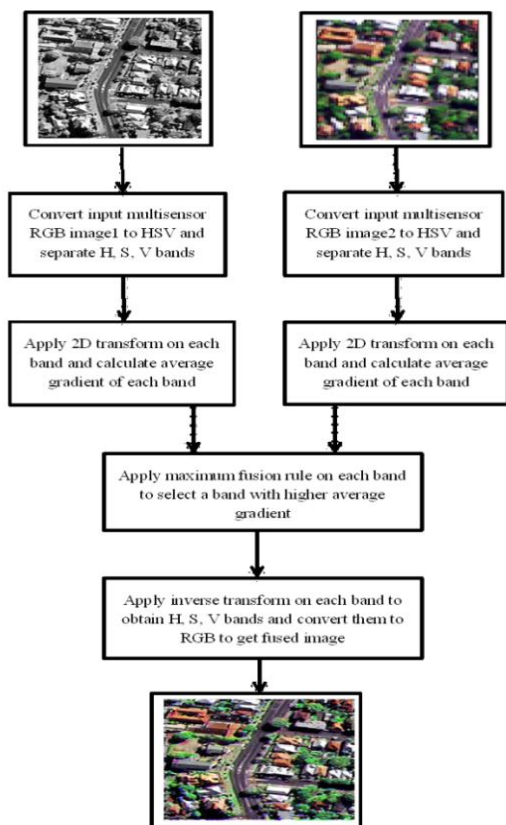

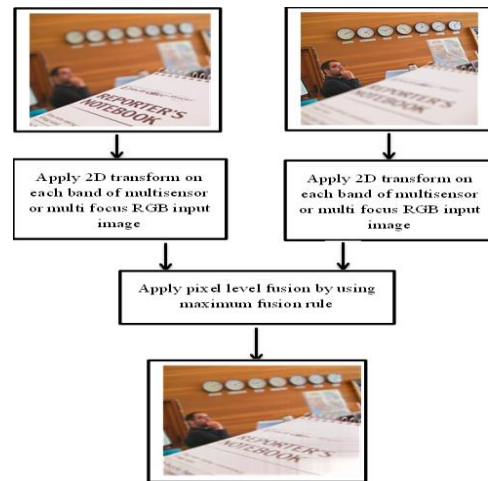**Figure 1: Block schematic for image fusion using a transform technique for multisensor RGB input images.**

Figure 2: Block schematic for image fusion using a transform technique for Multi-focus RGB or grayscale input images.

Algorithm 1: The common steps involved in the algorithm for image fusion of multisensor RGB input images are as follows:

1. Select two images from the data set.
2. Resize both images to 256x256.
3. Convert the RGB image into the HSV image. Now three bands are available, H, S, V.
4. Perform image fusion in the specific transform domain.
5. Convert HSV image into RGB for resultant image.

Algorithm 2: The common steps involved in the algorithm for image fusion of Multi-focus RGB or grayscale input images are as follows:

1. Select two images from the data set.
2. Resize images to 256x256.
3. If it is a color image, then it is divided into R, G, B planes.
4. Perform image fusion in the specific transform domain.

IV. RESULT AND DISCUSSIONS

Here two input images are panchromatic and multispectral. In the panchromatic image, objects are clear but at grayscale, whereas in multispectral, color information is given but objects are a blur. To get both the information, image fusion is done by using the proposed transform methods on two sets of images. Fig. 3 shows the image fusion for test set 1 of multisensor RGB images. The images obtained by HDCT, HDST, HWT methods in Fig. 3 (c), (f), (g) respectively are very similar. The HKT method output i.e. Fig. 3 (e) is observed better. The upper part of the image is more informative than the lower part whereas in Fig. 3 (d), i. e. the output obtained using HDWT, the objects are more clear but color information is not properly reflected.

The above discussion is a part of subjective analysis. The objective analysis is done by quality metrics. Table 1 shows quality metrics for the fused image obtained using different techniques for test set 1 of multisensor RGB images. Ten parameters are included to find the consistency of the fused image using various methods.
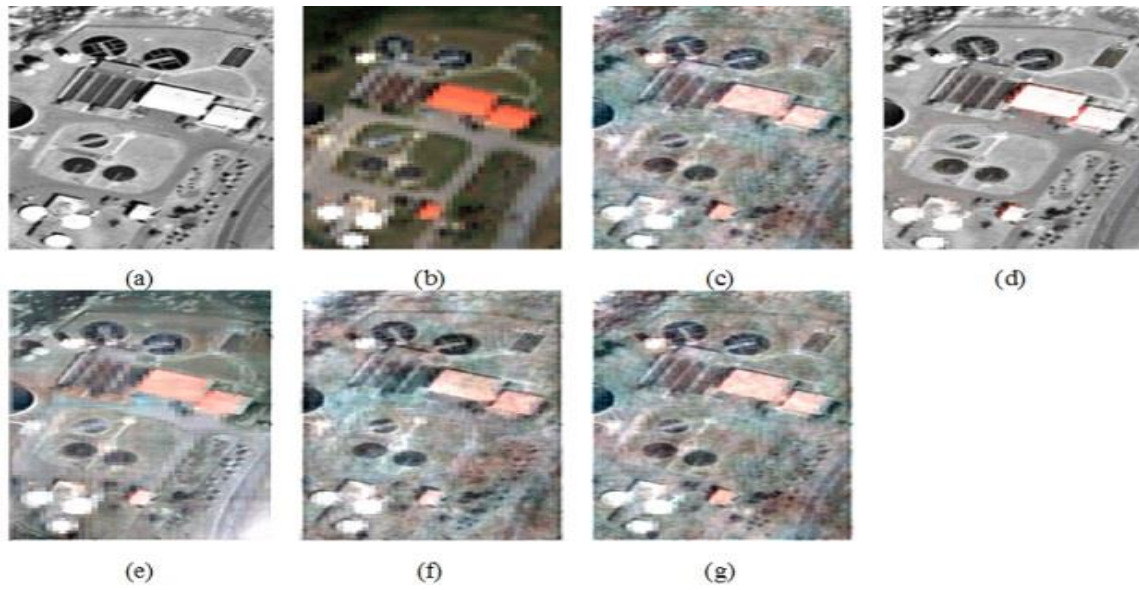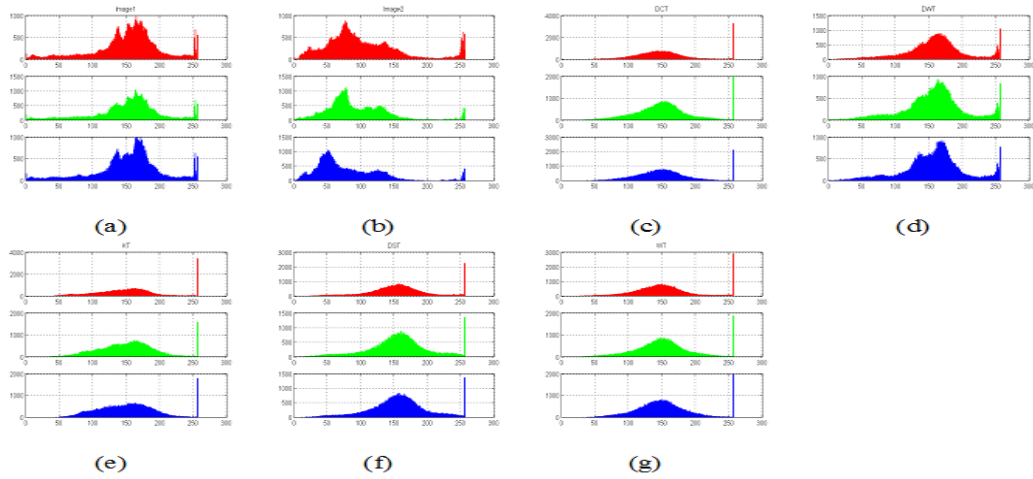

Figure 3: Image fusion for test set 1 of multisensor RGB images. (a) and (b) are input images from different sensors, (c) to (g) are fused images obtained using different hybrid transform methods as (c) HDCT, (d) HDWT, (e) HKT, (f) HDST, and (g) HWT.

Table 1 Performance parameters of image fusion using different hybrid transform techniques for test set 1 of the multisensor RGB image.

Quality Metrics	HDCT	HDWT	HKT	HDST	HWT
Mean	117.46	**128.63**	117.38	116.02	119.64
Entropy	7.32	**7.57**	7.31	7.28	7.38
Var	3416.63	2501.65	3459.36	3537.19	3268.41
Std Dev	58.45	50.02	58.82	59.47	57.17
RMSE	50.37	55.43	53.95	55.52	**25.26**
PSNR	32.51	30.59	31.13	30.56	**46.31**
SF	21.70	25.22	22.28	23.41	24.66
MI	1.65	1.07	1.65	1.64	1.67
IQI	0.10	-0.02	0.10	0.11	0.08
AG	25.82	18.44	25.41	26.77	24.60

The Mean is a good predictor of visual quality and is higher in HDWT. Entropy value reflects the information contents in the fused image. This is also good in HDWT. RMSE and PSNR are superior in HWT compared to other methods. The third method of analysis is histogram representation. The histogram is nothing but a graphical representation showing the total number of pixels with different intensities in an image. Here, the histogram of input and output images is drawn. Fig. 4 shows the histogram representation of input images from test set 1 of the multisensor RGB image and the fused image obtained by different hybrid transform techniques.

Figure 4: **(a) and (b) are the histogram of multisensor RGB input images from the test set 1, (c) to (g) are the histogram of fused images obtained using different hybrid transform methods as (c) HDCT, (d) HDWT, (e) HKT, (f) HDST, and (g) HWT.**

In Fig. 4, (a) is the histogram of the panchromatic image and (b) is the histogram of a multispectral image in the dark and hence towards the left side. The histogram in Fig. 4 (c), (e), (f), and (g) are very much close to each other. The number of highest value pixels in these histograms is near 2000. But in (d), the high frequency and low-frequency pixel distribution are the same as available in input images.
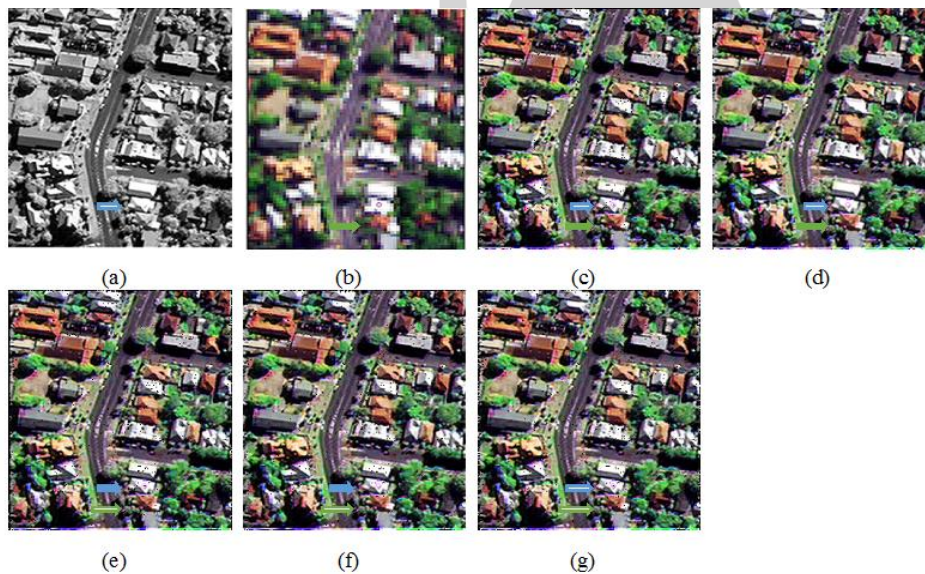
Figure 5: Image fusion for test set 2 of multisensor images. (a) and (b) are the input images from different sensors, (c) to (g) are fused images obtained using different hybrid transform methods as (c) HDCT, (d) HDWT, (e) HKT, (f) HDST, and (g) HWT.

In Fig 5, all images are visually clear but (c), (e), (f), and (g) have some additive noise. In Fig. 5 (a), the white roof of the house shown by the blue arrow should be as it is in the fused image but in (c), (e), (f), and (g), the noise is available. This is reflected by black dots on the white roof. Another observation is about the orange circle on the white roof shown by an orange arrow. For this also, in (c), (e), (f), and (g), the noise is available with the said object but in (d), we can observe the object clearly without any noise. Table 2 shows quality metrics for the fused image obtained using different techniques for test set 2 of satellite multisensor RGB images. From this table, the RMSE and PSNR are good in HDWT compared to other methods. Fig. 6 shows the histogram representation of input images from the test set 2 of the multisensor RGB image and fused image obtained by different hybrid transform methods. The histograms of these fused images are very much similar to each other as well as with input images.

Table 2 Performance parameters of image fusion using different hybrid transform techniques for test set 2 of the multisensor RGB image.

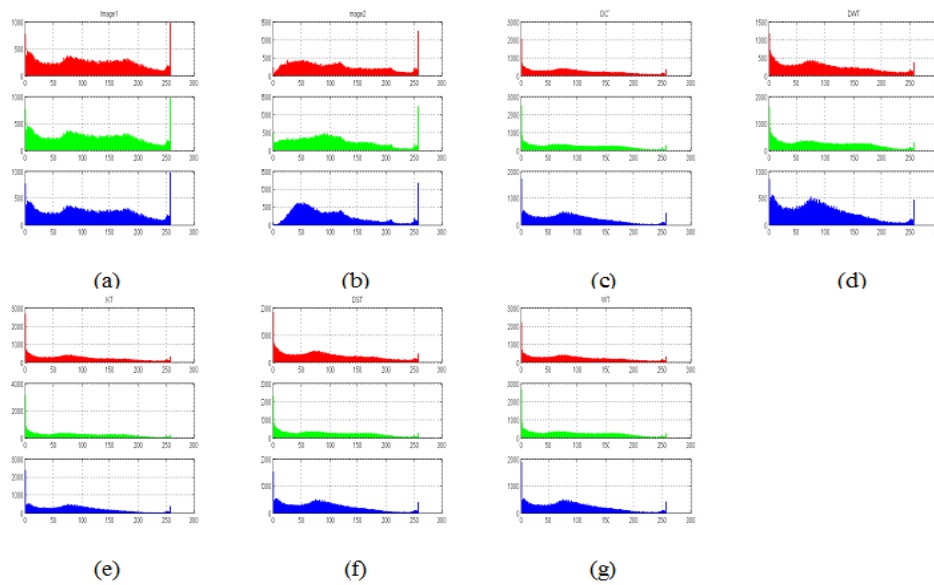| Quality Metrics	HDCT	HDWT	HKT	HDST	HWT
Mean	93.52	94.98	92.34	93.74	93.16
Entropy	7.77	7.81	7.74	7.78	7.77
Var	4482.51	4435.30	4496.10	4455.11	4479.60
Std Dev	66.95	66.60	67.05	66.75	66.93
RMSE	34.99	**29.70**	37.94	34.89	36.04
PSNR	39.80	**42.92**	38.19	39.86	39.21
SF	50.11	43.36	52.28	49.86	51.38
MI	1.94	**1.98**	1.93	1.95	1.94
IQI	0.98	0.99	-0.89	0.98	-0.89
AG	20.69	19.62	20.80	20.43	20.66

Figure 6: (a) and (b) are the histogram of multisensor input images from Test set 2, (c) to (g) are the histogram of fused images obtained by different hybrid transform methods as (c) HDCT, (d) HDWT, (e) HKT, (f) HDST, and (g) HWT.

Table 3 shows the comparison of quality metrics for the fused image obtained using different techniques for test set 2 of satellite multisensor RGB images and existing methods given in references. The quality metrics are given in reference papers taken as it is in table 3.

Table 3 Comparison of quality metrics due to hybrid transforms method and existing methods for a multisensor RGB input image.

Quality Metrics	HDCT	HDWT	HKT	Ref.6	Ref.16	Ref.18
Mean	93.52	94.98	92.34			
Entropy	7.77	7.81	7.74		6.65	
Var	4482.51	4435.30	4496.10			
Std Dev	66.95	66.60	67.05		54.54	57.07
RMSE	34.99	29.70	37.94	0.09		
PSNR	39.80	42.92	38.19	93.8	4.56	
SF	50.11	43.36	52.28			
MI	1.94	1.98	1.93	0.9		8.64
IQI	0.98	0.99	-0.89	0.8		0.76
AG	20.69	19.62	20.80			

The entropy of resultant images by the proposed hybrid transform technique is better than the technique given in ref. 16. IQI is also good in HDCT and HDWT compared to the method given in ref. 6 and 18 but RMSE and PSNR are superior in ref. 6.

In multi-focus image fusion, the images of focus on different objects are used. In the test set 1, in the first image, the focus is on a book, and in the second image focus is on the man and clock.
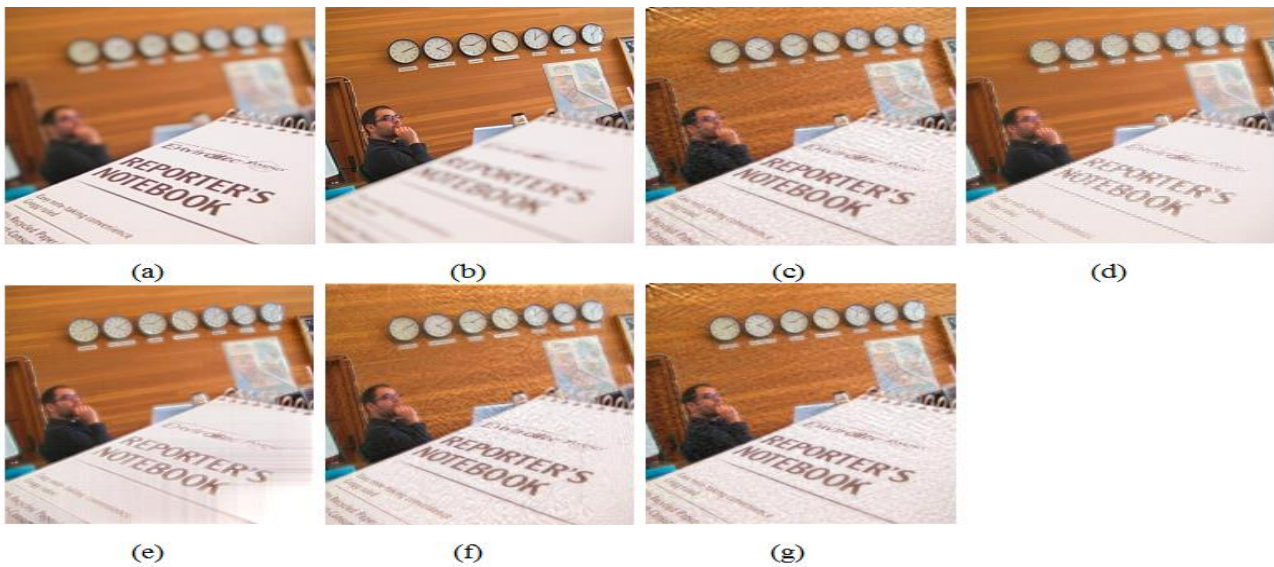
Figure 7: Image fusion for test set 1 of multi-focus images. (a) and (b) are input images at different focuses, (c) to (g) are fused images obtained using different hybrid transform methods as (c) HDCT, (d) HDWT, (e) HKT, (f) HDST, and (g) HWT.

The fused output image obtained by using different hybrid transform techniques is given in Fig. 7 (c) to (g). After visual observation, all images are blurred. But comparison among them reflects that the fused image of HKT is better than other methods with some effect on the bottom right side of the image. Table 4 shows quality metrics for the fused image obtained using different techniques for test set 1 of multi-focus RGB images. The RMSE and PSNR are very good in the fused image obtained by HWT.

Table 4 Performance parameters of image fusion using different hybrid transform techniques for test set 1 of the multi-focus RGB image.

Quality Metrics	HDCT	HDWT	HKT	HDST	HWT
Mean	150.04	138.35	150.85	148.52	151.21
Entropy	7.42	7.33	7.47	7.40	7.42
Var	5297.15	3639.32	5125.33	5414.49	5205.10
Std dev	72.78	60.33	71.59	73.58	72.15
RMSE	11.44	13.42	13.19	12.51	**8.03**
PSNR	62.17	58.97	59.31	60.38	**69.25**
SF	16.17	16.16	13.86	16.57	16.93
MI	3.96	3.21	3.51	3.94	3.97
IQI	-0.63	0.94	0.98	0.94	0.95
AG	10.75	6.25	10.39	11.80	10.09

In test set 2, in the first image, the focus is on the calendar, and in the second image, the focus is on the book. The fused output image obtained by using different hybrid transform techniques is given in Fig. 8 (c) to (g).

Figure 8: Image fusion for test set 2 of multi-focus images. (a) and (b) are input images at different focuses, (c) to (g) are fused images obtained using different hybrid transform methods as (c) HDCT, (d) HDWT, (e) HKT, (f) HDST, and (g) HWT.

Fig. 8 (d) is clearer than the other fused images. This is the output of the HDWT method whereas the fused output obtained by the HKT method is nearer to the output of HDWT. The output obtained by HDCT and HDST is very similar to each other. Table 5 shows quality metrics for the fused image obtained using different techniques for test set 2 of multi-focus RGB images. In this table also, in the HWT method, RMSE and PSNR values are far better than the other methods.

Table 5 Performance parameters of image fusion using different hybrid transform techniques for test set 2 of the multi-focus RGB image.

Quality Metrics	HDCT	HDWT	HKT	HDST	HWT
Mean	67.45	51.16	66.66	65.72	67.96
Entropy	6.18	5.82	6.20	6.16	6.13
Var	3812.52	2287.25	3835.26	3820.40	3811.21
Std dev	61.75	47.83	61.93	61.81	61.73
RMSE	11.65	13.30	13.18	13.34	**8.34**
PSNR	61.80	59.15	59.33	59.09	**68.47**
SF	10.63	12.31	10.38	11.07	11.68
MI	4.14	3.14	3.26	3.22	4.22
IQI	0.99	0.89	0.99	0.99	0.99
AG	3.14	2.84	3.47	3.84	2.74

Table 6 Comparison of quality metrics due to hybrid transforms method and existing methods for the multi-focus RGB input image.

Quality Metrics	HDCT	HDWT	HKT	Ref. 9	Ref. 22	Ref. 24
Mean	150.04	138.35	150.85			
Entropy	**7.42**	7.33	**7.47**	7.39		5.14
Var	5297.15	3639.32	5125.33			
Std dev	72.78	60.33	71.59	51.94		55.23
RMSE	11.44	13.42	13.19			
PSNR	62.17	58.97	59.31		24.82	25.21
SF	16.17	16.16	13.86	**22.23**		
MI	3.96	3.21	3.51			**6.97**
IQI	-0.63	0.94	0.98		0.16	
AG	10.75	6.25	10.39			

Table 6 represents the difference in quality metrics due to the hybrid transforms method and existing methods for the multi-focus RGB input image. In ref. 9, two types of parameters are used. Reference-based parameters are RMSE, MI, and PSNR, and non-reference-based parameters are SF, SD, and Entropy. The proposed technique is also not using any reference image so non-reference-based parameters are compared only. Among these, SF is superior to the proposed techniques. In ref. 22, the technique is based on the DWT-GA transformation. The PSNR and IQI are compared and demonstrate that the suggested hybrid transform technique is giving a better result. In ref. 24, the MI is superior to other parameters.

Another set of multisensor image fusion is from medical imaging. In the following set of examples, medical images are from different sensors. The image of a particular body part is captured through different sensors. Fig. 9 shows the image fusion for test set 1 of multisensor medical images**.**
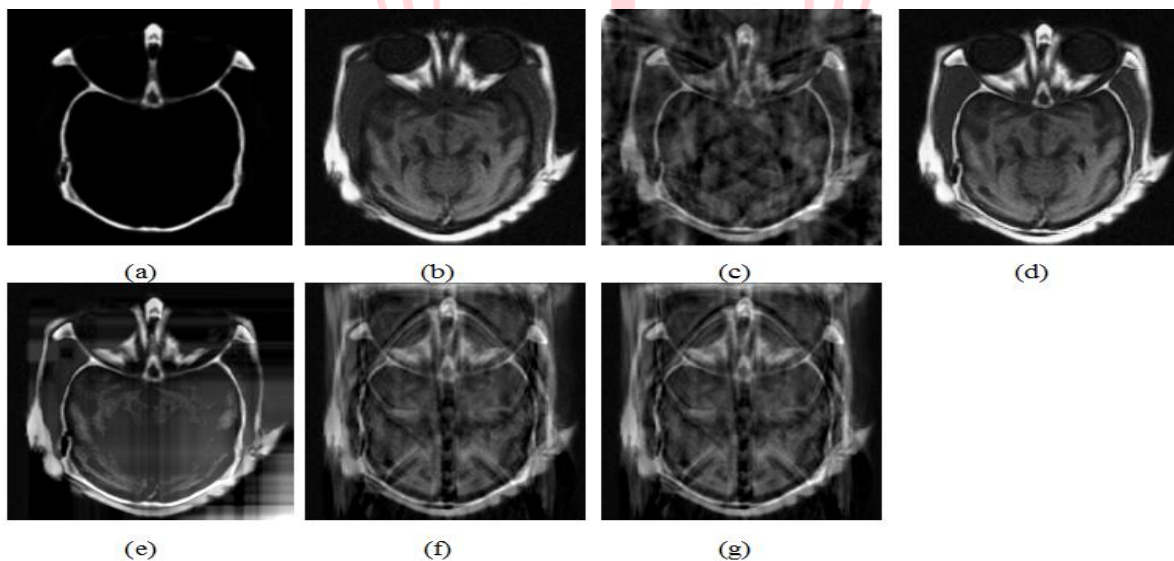
Figure 9: Image fusion for test set 1 of multisensor medical images. (a) and (b) are input images from different sensors, (c) to (g) are fused images obtained using different hybrid transform methods (c) HDCT, (d) HDWT, (e) HKT, (f) HDST, and (g) HWT.

It is observed that the output obtained by HDWT is showing inner parts more clearly. The fused image obtained by HDCT, HDST, and HWT is blurred. The image obtained by HKT is partially clear. The bottom right part of this image is blurred. Table 7 shows quality metrics for the fused image obtained using different techniques for test set 1 of multisensor medical images.

Table 7 Performance parameters of image fusion using different hybrid transform techniques for Test set 1 of multisensor medical image.

Quality Metrics	HDCT	HDWT	HKT	HDST	HWT
Mean	52.67	58.75	10.10	57.30	52.67
Entropy	6.91	6.86	1.71	7.11	6.92
Var	1845.60	3520.20	1310.92	1851.72	1941.50
Std dev	42.96	59.33	36.21	43.03	44.06
RMSE	59.78	73.09	63.12	64.29	59.83
PSNR	29.09	24.91	28.00	27.64	29.07
SF	13.60	**17.77**	16.14	12.45	19.26
MI	0.52	**1.40**	0.99	0.59	0.52
IQI	0.55	0.56	0.58	0.56	0.55
AG	5.45	6.44	2.76	5.83	6.85

After visual observation, the output obtained by HDWT is clearer, and the same is reflected through quality metrics. The SF and MI in HDWT are superior to other methods. Thus we can observe fine details in the fused image. Fig. 10 shows the histogram of images obtained by using hybrid transform techniques for test set 1 of multisensor medical images.

From Fig. 10, the histogram of the input image i.e. (b), and histogram of the fused image obtained by HDWT i.e.(d) is matching. The histogram of the fused image obtained by other methods is not matching with input image histograms. Fig. 11 shows the fused images for test set 2 of multisensor medical images.
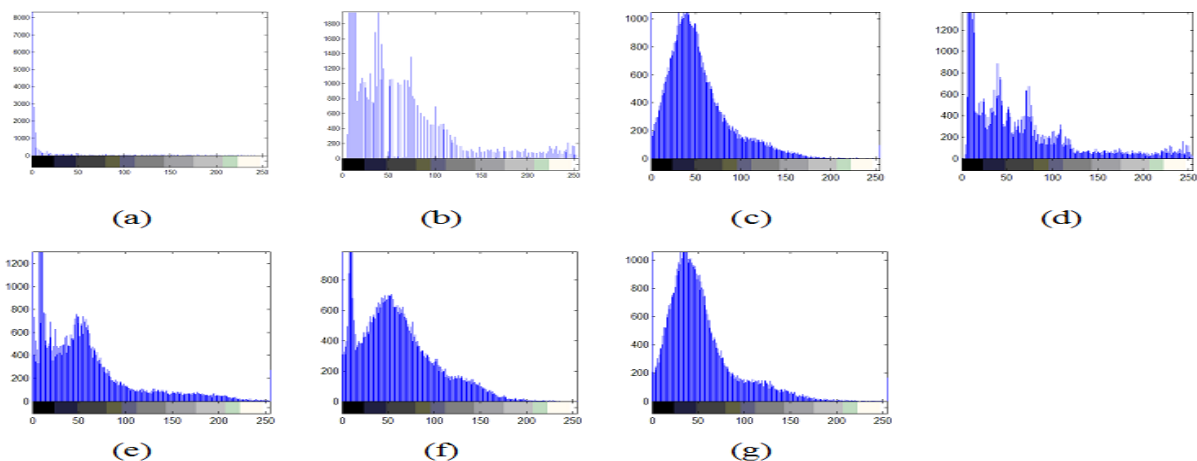

Figure 10: (a) and (b) are the histogram of multisensor medical input images from the test set 1, (c) to (g) are the histogram of fused images obtained using different hybrid transform methods (c) HDCT, (d) HDWT, (e) HKT, (f) HDST, and (g) HWT.
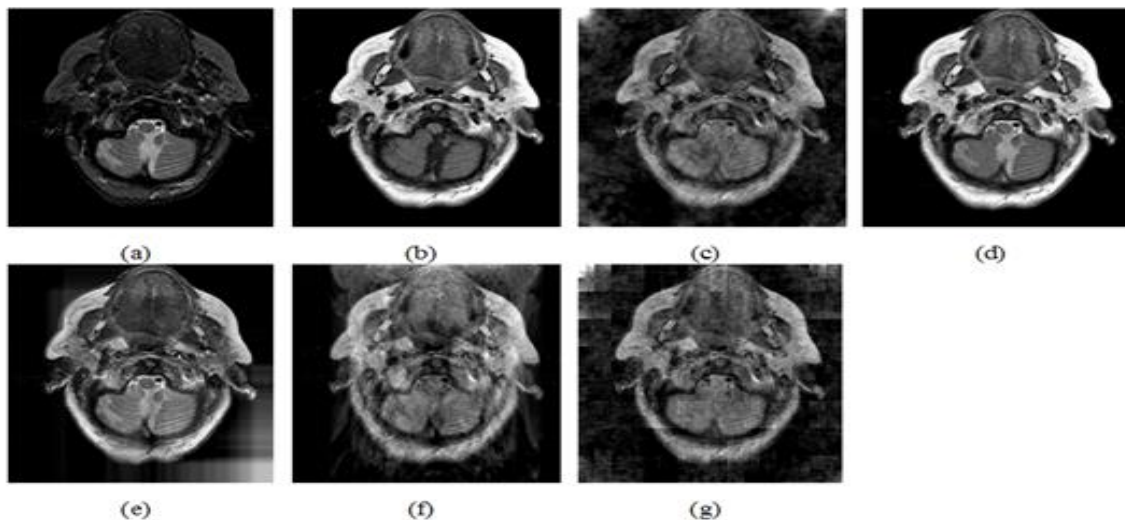

Figure 11: Image fusion for test set 2 of multisensor medical images. (a) and (b) are input images from different sensors, (c) to (g) are fused images obtained using different hybrid transform methods (c) HDCT, (d) HDWT, (e) HKT, (f) HDST, and (g) HWT.

Here also, it is observed that the output image obtained by HDWT is showing the complete fusion of input images. Whereas in HKT, the fused image is nearer to complete fusion. But the fused image obtained by HDCT, HDST, and HWT is blurred. Table 8 shows the performance parameters for test set 2 of multisensor medical images.

Table 8 Performance parameters of image fusion using different hybrid transform techniques for test set 2 of multisensor medical image.

Quality Metrics	HDCT	HDWT	HKT	HDST	HWT
Mean	57.06	61.13	21.87	61.96	57.06
Entropy	7.10	5.55	4.60	6.71	7.07
Var	2730.03	5458.31	1064.85	3470.51	2837.09
Std dev	52.25	73.88	32.63	58.91	53.26
RMSE	54.43	70.17	56.67	61.29	54.87
PSNR	30.97	25.73	30.16	28.59	30.80
SF	17.93	**22.45**	18.81	16.10	21.50
MI	1.11	**1.59**	**2.89**	1.18	1.10
IQI	0.75	0.70	0.72	0.70	-0.73
AG	6.94	7.40	4.64	6.74	7.79

Table 9 Comparison of quality metrics due to hybrid transforms method and existing methods for the multisensor medical input image.

Quality Metrics	HDCT	HDWT	HKT	Ref. 19
Mean	52.67	58.75	10.10	
Entropy	6.91	6.86	1.71	**8.81**
Var	1845.60	3520.20	1310.92	
Std dev	42.96	59.33	36.21	
RMSE	59.78	73.09	63.12	3.31
PSNR	29.09	24.91	28.00	41.91
SF	13.60	17.77	16.14	
MI	0.52	1.40	0.99	**7.44**
IQI	0.55	0.56	0.58	**0.85**
AG	5.45	6.44	2.76	

From table 8 also, the quality metrics SF and MI are good in HDWT. Table 9 shows the comparison of quality metrics due to the hybrid transforms method and existing methods for the multisensor medical input image. In ref. 19, the hybridization is done by using wavelet and curvelet transform. RMSE and PSNR are not considered for comparison because in ref. 19, the reference image is used to find RMSE. But by comparing entropy and MI, these parameters are superior in ref. 19.

In night vision applications, images captured by the IR sensor are very useful. The multisensor night vision image fusion in which input images are captured from IR and CCD camera. Fig. 12 shows image fusion for test set 1 of multisensor night vision images.
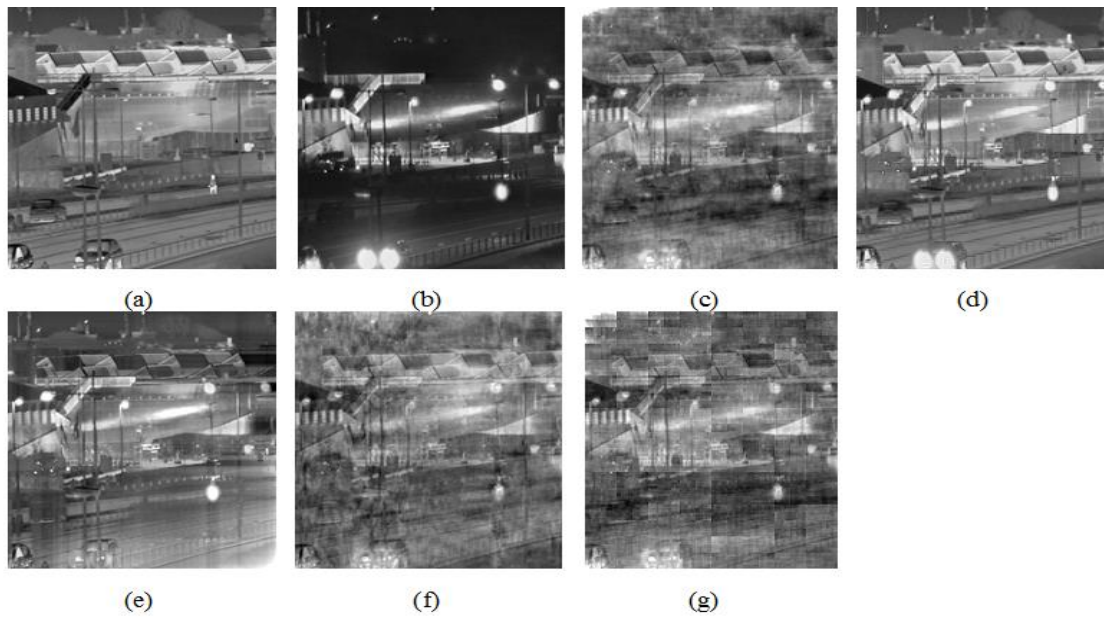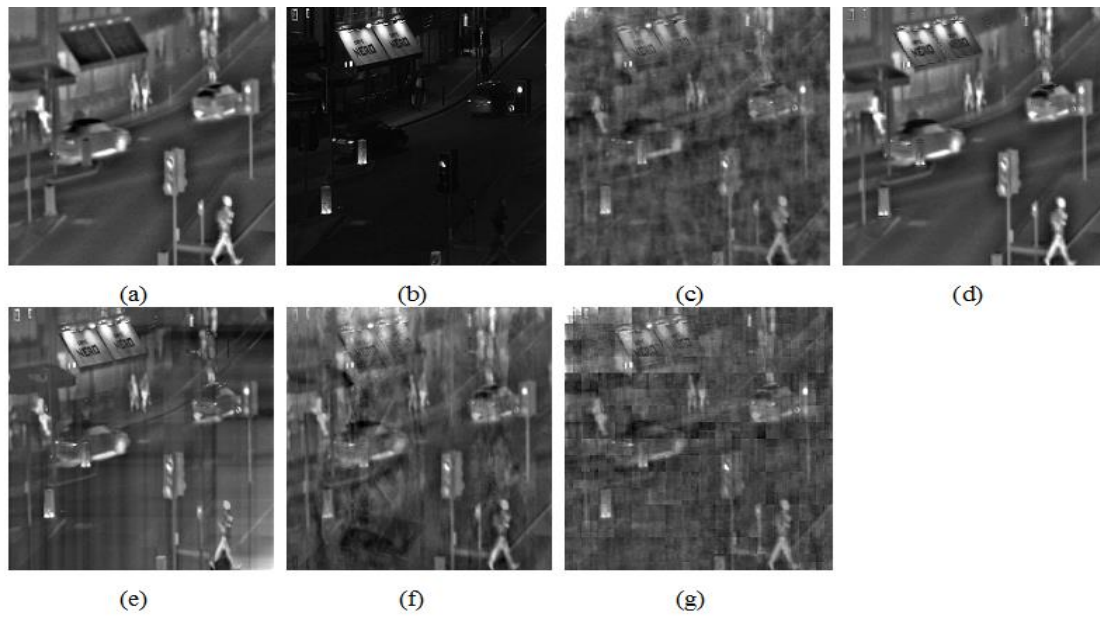
Figure 12: Image fusion for test set 1 of multisensor night vision images. (a) and (b) are input images from different sensors at night, (c) to (g) are fused images obtained using different hybrid transform methods (c) HDCT, (d) HDWT, (e) HKT, (f) HDST, and (g) HWT.

Fig. 12 (a) is the image from the IR camera which is difficult to interpret. And Fig. 12 (b) is the image from the CCD camera where objects are not properly visible. The fused image obtained by HDWT is more clear than the HDCT, DST, and HWT methods. The image obtained by HKT is also good but blurred at the bottom side. Table 10 shows the performance parameters of image fusion using different hybrid transform techniques for test set 1 multisensor night vision image.

Table 10 Performance parameters of image fusion using different hybrid transform techniques for test set 1 multisensor night vision image.

| Quality Metrics	HDCT	HDWT	HKT	HDST	HWT
Mean	111.64	119.73	111.64	114.98	111.64
Entropy	7.28	7.31	7.17	7.12	7.25
Var	1892.76	1895.05	1482.56	1222.51	1756.92
Std dev	43.51	43.53	38.50	34.96	41.92
RMSE	42.73	**27.97**	44.85	30.46	42.08
PSNR	35.80	**44.12**	34.84	42.58	36.11
SF	17.22	**20.14**	18.02	15.25	20.00
MI	0.83	1.25	**3.92**	0.74	0.81
IQI	0.81	0.58	0.76	0.66	0.80
AG	6.79	7.39	6.87	7.21	7.61

Figure 13: Image fusion for test set 2 of multisensor night vision images. (a) and (b) are input images from different sensors at night, (c) to (g) are fused images obtained using different hybrid transform methods as (c) HDCT, (d) HDWT, (e) HKT, (f) HDST, and (g) HWT.

From table 10 also, it is observed that HDWT and HKT are better than HDCT, HDST, and HWT. Figure 13 shows the image fusion for test set 2 of multisensor night vision images. And table 11 shows the performance parameters of image fusion using different hybrid transform techniques for Test set 2 multisensor night vision image.

Table 11 Performance parameters of image fusion using different hybrid transform techniques for test set 2 multisensor night vision image.

Quality Metrics	HDCT	HDWT	HKT	HDST	HWT
Mean	80.92	83.85	80.92	82.51	80.92
Entropy	6.47	6.76	6.72	6.89	6.50
Var	905.16	1257.36	1074.76	1075.53	951.46
Std dev	30.09	35.46	32.78	32.80	30.85
RMSE	30.61	**18.74**	32.12	25.55	30.43
PSNR	42.48	**52.14**	41.52	46.09	42.60
SF	13.01	**15.80**	12.23	12.20	16.06
MI	0.56	1.17	**3.59**	0.76	0.60
IQI	0.46	0.07	0.50	0.23	0.22
AG	4.73	5.38	4.90	5.36	5.63

From Fig. 13 and table 11 also, it is observed that HDWT and HKT are superior to HDCT, HDST, and HKT for multisensor night vision image fusion. Now all these proposed hybrid methods are compared by graphical representation of performance parameters. Fig. 14 shows the graphical representation of RMSE, PSNR SF, MI, IQI, and AG of fused images for all test sets.
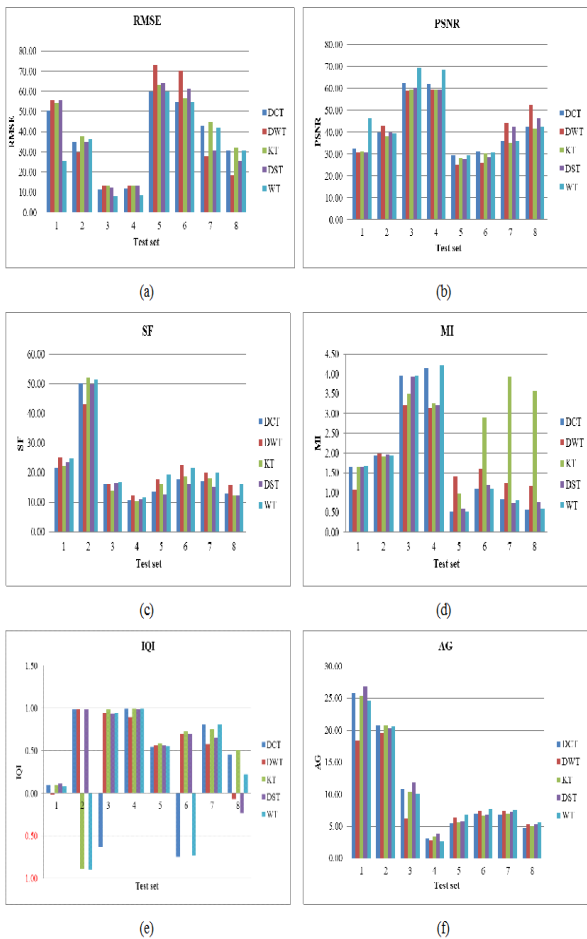
Figure 14: Graphical representation of a) RMSE b) PSNR c) SF d) MI e) IQI f) AG of fused images for all test sets.

5. CONCLUSIONS

The proposed hybrid transform method is the combination of HSV transform from spatial domain and one of the transforms among DCT, DWT, KT, DST, WT from transform domain. The performance of these methods is tested on four types of input sets by three different modes i. e. visually, through quality metrics, and histogram representation. In multisensor RGB input type, for test set 1 only HDWT is giving better performance but for test set 2, all methods are giving better performance. This is because the input image from test set 2 includes more color information. And due to HSV conversion, all transforms reflects the complete fused image. In multifocus RGB input type, visually HDWT and HKT are good but through quality metrics, the HWT method is superior. In the multisensor medical image set, HDWT shows better performance through all three modes. In multisensor night vision input types, HDWT and HKT are superior to other methods. So overall for any input type, HDWT and HKT are giving better performance. But by observing the output images of these methods as well as quality metrics, the output can be optimized. The next chapter is the optimization technique to enhance the efficiency of the fused image.

CONFLICT OF INTEREST: The authors declare that they have no conflict of interest.

REFERENCES

[1] Krista Amolins, Yun Zhang, and Peter Dare, "Applications of wavelet transforms in image fusion", IEEE Urban remote sensing joint event, 2007.

[2] Gaurav Bhatnagar, and Balasubramanian Raman, "A new image fusion technique based on directive contrast", Electronic letters on computer vision and image analysis, vol. 8, no. 2, pp. 18-38, 2009.

[3] Chaunte W Lacewell, Mohamed Gebril, Ruben Buaba, and Abdollah Homaifar, "Optimization of image fusion using genetic algorithms and discrete wavelet transform", IEEE Aerospace and Electronics Conference, pp. 116-121, July 2010.

[4] H. B. Kekre, Dhirendra Mishra, and Rakhee Saboo, "Review on image fusion techniques and performance evaluation parameters", International Journal of Engineering Science and Technology, vol. 5, no. 4, April 2013.

[5] Liu Cao, Longxu Jin, Hongjiang Tao, Guoning Li, Zhuang Zhuang, and Yanfu Zhang, "Multi-Focus image fusion based on spatial frequency in discrete cosine transform domain", IEEE signal processing letters, vol. 22, no. 2, pp. 220-224, February 2015.

[6] Joy Jinju, N. Santhi, K. Ramar, and B. Sathya Bama, "Spatial frequency discrete wavelet transform image fusion technique for remote sensing applications", Engineering Science and Technology, vol. 22, pp. 715–726, 2019.

[7] J. J. Lewis, R. J. O'Callaghan, S. G. Nikolov, D. R. Bull, and C. N. Canagarajah, "Region-based image fusion using complex wavelets", Information fusion, vol. 8, no. 2, pp. 119-130, 2007.

[8] Y. Asnath Victy Phamila, and R. Amrutha, "Discrete cosine transform based fusion of multi-focus images for visual sensor networks", Signal Processing, vol. 95, pp. 161-170, 2014.

[9] Vaibhav R. Pandit, and R. J. Bhiwani, "Image fusion in remote sensing applications: A review", International Journal of Computer Applications, vol. 120, no. 10, pp. 22-32, June 2015.

[10] Jiang Dong, Dafang Zhuang, Yaohuan Huang, and Jingying Fu, "Advances in Multi-Sensor Data Fusion: Algorithms and Applications", Sensors, vol. 9, pp. 7771-7784, 2009.

[11] Srinivasa Rao Dammavalam, Seetha Maddala, and Krishna Prasad MHM, "Quality Assessment of Pixel-Level Image Fusion using Fuzzy Logic", International

Journal on Soft Computing, vol. 3, no. 1, pp. 13-25, February 2012.

[12] harath H. Aithal, Uttam Kumar, and Ramachandra T.V., "Fusion of multi-resolution remote sensing data for urban sprawl analysis", COSMAR 09, Indian Institute of Science, 2009.

[13] Geun-Young Lee, Sung-Hak Lee, and Hyuk-Ju Kwon, "DCT-Based HDR Exposure Fusion Using Multiexposed Image Sensors", Hindawi Journal of Sensors, vol. 2017, pp.1-14, December 2017.

[14] B. L. N. Kennett, "A note on finite walsh transform", IEEE Transaction on Information Theory, pp. 489-490, July 1970.

[15] Liu Shangzheng, Han Jiuqiang, Bowen Liu, and Zhang Xinman, "An image fusion algorithm based on polyharmonic local sine transform (PHLST), Optica Applicata, vol. XXXIX, no. 2, pp. 347-356, 2009.

[16] M. Divya, S. Aruna Mastani, and VPS Naidu, " Real Time Image Fusion using Multi Resolution Discrete Sine Transform" Int. Journal of Engineering Research and Application, vol. 7, issue 11, pp. 55-60, November 2017.

[17] Jingming Xia, Yi Lu, and Ling Tan, "Research of Multimodal Medical Image Fusion Based on Parameter-Adaptive Pulse-Coupled Neural Network and Convolutional Sparse Representation", Hindawi Computational and Mathematical Methods in Medicine, vol. 2020, pp. 1-13, 2020.

[18] Lin He, Xiaomin Yang, Lu Lu, WeiWu, Awais Ahmad, and Gwanggil Jeon, "A novel multi-focus image fusion method for improving imaging systems by using cascade-forest model", EURASIP Journal on Image and Video Processing, pp. 1-14, 2020.

[19] Jyoti Agarwal, and Sarabjeet Singh Bedi, "Implementation of hybrid image fusion technique for feature enhancement in medical diagnosis", Human-centric Computing and Information Sciences, pp. 1-17, 2015.

[20] VPS Naidu, "Discrete Cosine Transform based Image Fusion Techniques", vol. 1, no. 1, pp. 35-45, Journal of Communication, Navigation and Signal Processing, vol. 1. No. 1, pp. 35-45, January 2012.

[21] Sujoy Paul, Ioana S. Sevcenco, and Panajotis Agathoklis, "Multi-Exposure and Multi-Focus Image Fusion in Gradient Domain", Journal of Circuits, Systems, and Computers, vol. 25, no. 10, pp. 1650123-1:18, 2016.

[22] Yuanmeng Zhao, Yulong Qiao, Cunlin Zhang, Yuejin Zhao, and Hong Wu, "Terahertz /Visible Dual-band Image Fusion Based on Hybrid Principal Component Analysis", Journal of Physics: Conference Series 1187, pp. 1-5, 2019.

[23] Naoto Yokoya, Takehisa Yairi, and Akira Iwasaki, "Coupled nonnegative matrix factorization unmixing for hyperspectral and multispectral data fusion", IEEE transactions on geoscience and remote sensing, vol. 50, no. 2, pp. 528-537, February 2012.

[24] Syed Sohaib Ali, Muhammad Mohsin Riaz, and Abdul Ghafoor, "Hybrid Component Substitution and Wavelet Based Image Fusion", IEEE conference in Acoustics, Speech, and Signal Processing, pp. 2498-2502, October 2013.

[25] Suhas Lohit, Dehong Liu, Hassan Mansour, and Petros T. Boufounos, "Unrolled Projected Gradient Descent for Multi-Spectral Image Fusion", IEEE conference in Acoustics, Speech, and Signal Processing, March 2019.

[26] Dunbin Shen, Jianjun Liu, Zhiyong Xiao, Jinlong Yang, and Liang Xiao, "A Twice Optimizing Net With Matrix Decomposition for Hyperspectral and Multispectral Image Fusion", IEEE Journal of Selected Topics in Applied Earth Observations and Remote Sensing, vol. 13, pp. 4095-4110, 2020.

[27] Zhaoyang Ji, Xudong Kang, Kunzhong Zhang, Puhong Duan, And Qiaobo Hao, "A Two-Stage Multi-Focus Image Fusion Framework Robust to Image Mis-Registration", vol. 7, pp. 123231-123243, 2019.

[28] Qi Xie, Minghao Zhou, Qian Zhao, Deyu Meng, Wangmeng Zuo, Zongben Xu, "Multispectral and Hyperspectral Image Fusion by MS/HS Fusion Net", IEEE Conference on Computer Vision and Pattern Recognition, pp. 1585-1594, 2019.

[29] Aiqing Fang, Xinbo Zhao, Jiaqi Yang, Yanning Zhang, Jiaqi Yang, and Yanning Zhang, "A Cross-Modal Image Fusion Method Guided by Human Visual Characteristics", IEEE Transactions on Multimedia, pp. 1-13, June 2020.

[30] Benjamin Milgrom, Roy Avrahamy, Tal David, Avi Caspi, Yosef Golovachev, and Shlomo Engelberg, "Extended depth-of-field imaging employing integrated binary phase pupil mask and principal component analysis image fusion", Optics Express, vol. 28, no. 16 / 3, pp. 23862-23873, August 2020.

[31] Muhammad Shahid Farid, Arif Mahmood, Somaya Ali Al-Maadeed, "Multi-focus Image Fusion Using Content Adaptive Blurring", Information Fusion, pp. 1-17, February 2018.